ACS Medicinal Chemistry Letters
Cite This: ACS Med. Chem. Lett. 2019, 10, 209−214
Letter
pubs.acs.org/acsmedchemlett

Chromenopyrazole-based High Affinity, Selective Fluorescent Ligands for Cannabinoid Type 2 Receptor

Sameek Singh,[†] Caitlin R. M. Oyagawa,[§] Christa Macdonald,[§] Natasha L. Grimsey,[§] Michelle Glass,[§,∥] and Andrea J. Vernall*[,†]

[†]School of Pharmacy, University of Otago, Dunedin, New Zealand

[§]Department of Pharmacology and Clinical Pharmacology, and Centre for Brain Research, School of Medical Sciences, Faculty of Medical and Health Sciences, University of Auckland, Auckland, New Zealand

Supporting Information

ABSTRACT: Cannabinoid type 2 receptor (CB_2R) is an attractive target for the treatment of pain and inflammatory disorders. Availability of a selective CB_2R fluorescent ligand to study CB_2R expression and localization in healthy and disease conditions would greatly contribute to improving our understanding of this receptor. Herein, we report a series of chromenopyrazole-based CB_2R fluorescent ligands. The highest affinity fluorescent ligand was Cy5-containing **24** (hCB_2R pK_i = 7.38 ± 0.05), which had 131-fold selectivity over CB_1R. In a cAMP BRET assay, **24** behaved as a potent CB_2R inverse agonist. Widefield imaging experiments showed that **24** binds to CB_2R in live cells with good selectivity and low levels of nonspecific fluorescence. The high affinity, selectivity, and suitable imaging properties of fluorescent ligand **24** make it a valuable tool for studying CB_2R.

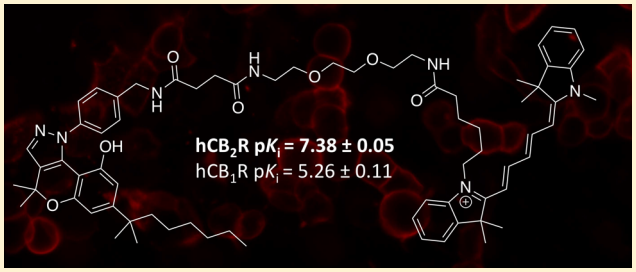

KEYWORDS: *GPCR, cannabinoid type 2 receptor, fluorescent ligand, chemical tool*

Cannabinoid receptors (CBRs) are Class A G protein-coupled receptors (GPCRs) with two defined subtypes: cannabinoid type 1 receptor (CB_1R) and cannabinoid type 2 receptor (CB_2R). CB_1R is abundantly expressed in the central nervous system, whereas CB_2R is mostly expressed in peripheral organs and cells such as spleen and immune cells.[1] CBRs are part of the endocannabinoid system and play an important role in a number of pathophysiological processes including pain, obesity, inflammation, and neurological disorders.[2] The development of CB_2R agonists for the treatment of pain and inflammatory diseases is an active area of research.[3,4] A number of CB_2R agonists have undergone clinical trials; however, many failed to show sufficient efficacy.[5] It would be advantageous if the expression level of CB_2R in different diseases and conditions was better understood.

There are several types of chemical tools commonly used to study GPCRs.[6] Very few selective CB_2R radioligands have been reported,[6,7] and to our knowledge, none are currently commercially available. Antibodies are in theory very selective; however, in practice many commercial fluorescent CB_2R antibodies have been shown to lack specificity for CB_2R.[6,8] Covalent ligands are useful tools in purification and crystallization of GPCRs as well as in probing ligand−receptor binding sites.[6] Fluorescent ligands are powerful tools to study GPCRs in a spatiotemporal manner in living native cells, with fluorescent agonists versus inverse agonist each having their own advantages and utilization.[6,9−12] Small molecule-based fluorescent ligands are usually prepared by covalent conjugation of a high affinity ligand to a fluorophore via a linker.[10] A fluorophore with excitation and emission >500 nm and a high quantum yield and extinction coefficient is desirable. The choice of fluorophore is often driven by a planned experiment, e.g., as a partner in a BRET assay.[13]

There are challenges associated with the development of a GPCR fluorescent ligand with suitable imaging properties. Conjugation of a linker and fluorophore to a ligand creates a new chemical entity that usually has different pharmacodynamic and physicochemical properties compared to the unconjugated ligand. In addition to good receptor affinity, a fluorescent ligand must also have low levels of nonspecific binding/interactions with other entities such as plasma membrane. A large proportion of CBR ligands are lipophilic (clogP > 5), making the development of a CBR fluorescent ligand with low levels of nonspecific membrane interactions challenging.

Fluorescent ligands for CB_2R prepared by conjugation of a ligand with fluorophore have been reported in the literature, most based on "mbc94", which is a derivative of the selective CB_2R ligand SR144528.[14,15] CB_2R fluorescent ligands based on indole[16] and naphthyridine[17] scaffolds have also been reported; however, these exhibited unsuitable affinity or

Received: November 29, 2018
Accepted: January 30, 2019
Published: January 30, 2019

DOI: 10.1021/acsmedchemlett.8b00597
ACS Med. Chem. Lett. 2019, 10, 209−214

imaging properties. "Two-step" photoaffinity fluorescent ligand LEI121 has recently been developed for CB_2R in which the fluorophore is covalently attached *in situ* in a second step.[18] However, while this holds great promise for receptor labeling, the irreversible covalent nature limits its application in kinetic assays. Another two-step probe was developed based on the classical cannabinoid-like HU210 (**1**,[19] Figure 1A), with high affinity for both CB_2R and CB_1R. Interestingly, a closely related analogue of **1** with an Alexa Fluor 488 fluorophore (**2**,[20] Figure 1A) instead of biotin was reported as a CB_1R selective fluorescent ligand, indicating fluorescent ligand CBR subtype selectivity can be achieved despite being based on a nonselective ligand core. We chose to develop fluorescent ligands using a chromenopyrazole[21−23] core (e.g., **3**−**6**, Figure 1B).

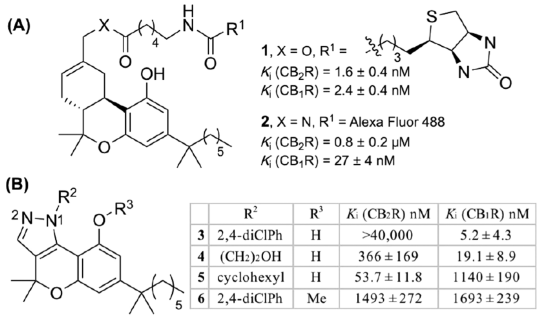

	R2	R3	Ki (CB2R) nM	Ki (CB1R) nM
3	2,4-diClPh	H	>40,000	5.2 ± 4.3
4	$(CH_2)_2OH$	H	366 ± 169	19.1 ± 8.9
5	cyclohexyl	H	53.7 ± 11.8	1140 ± 190
6	2,4-diClPh	Me	1493 ± 272	1693 ± 239

Figure 1. (A) Previously reported HU210-based probes with biotin (**1**),[19] Alexa Fluor 488 fluorophore (**2**),[20] and (B) previously reported chromenopyrazoles **3**−**6**.[21,22]

Structure−activity relationships (SARs) indicated the chromenopyrazole scaffold tolerates *N*-pyrazole aromatic (e.g., **3**) and alkyl (e.g., **4**,**5**) substituents, albeit resulting in CB_1R selective, CB_2R selective, or nonselective high affinity ligands.[21,22] Chromenopyrazole phenolic alkylation was reported to improve CB_2R selectivity;[22] however, *N*-phenyl and *O*-alkyl in the same ligand (e.g., **6** and six other examples in ref 22) led to a loss of CBR affinity. Therefore, in our study we developed a series of pyrazole-*N*-phenyl-linked fluorescent ligands with an unsubstituted phenol. Recently, Morales et al. reported a closely related chromenopyrazoledione scaffold conjugated to a porphyrin linked via the pyrazole nitrogen; however, this conjugate had very poor affinity for CB_2R.[24] As our ultimate goal was to develop a CB_2R selective tool, if the first series of fluorescent ligands did not have suitable selectivity we rationalized that CB_2R versus CB_1R selectivity could be tuned by modification of the linker and/or fluorophore.[25] Fluorophores were selected with an emission >500 nm and with a range of molecular size and charge.

Synthesis of *N*-phenyl-chromenopyrazoles began with condensation of *β*-ketoaldehyde **7** with 3- or 4-hydrazinobenzoic acid to provide methyl esters **8** and **9** (Scheme 1). Although two regioisomers are possible via condensation of asymmetric hydrazines with **7**, only the *N*1-pyrzole was detected and isolated. This was assigned based on NMR spectra that showed comparable ^1H (of H-3′) and ^{13}C (of C-3′) chemical shifts to *N*1 regioisomers reported by Cumella et al.,[21] and is also the most likely regioisomer due to steric and electronic factors. Hydrolysis of methyl esters **8** and **9** with LiOH provided carboxylic acids **10** and **11**, which were reacted with NH_4Cl and HBTU to give benzamides **12** and **13**, respectively. Reduction of **12** and **13** with $LiAlH_4$ provided

Scheme 1. Synthesis of *N*-Phenyl-chromenopyrazole Fluorescent Ligands[a]

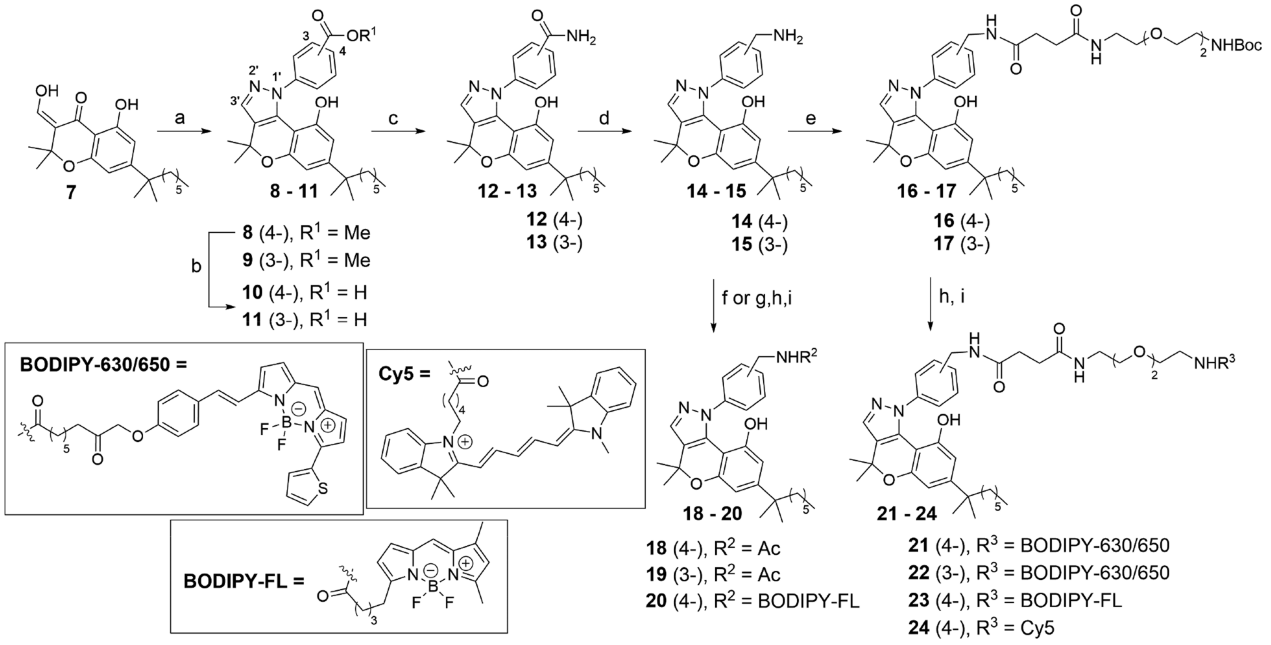

[a]Reagents and conditions: (a) 4-hydrazinobenzoic acid or 3-hydrazinobenzoic acid HCl, H_2SO_4, MeOH, 75 °C, 8 h, 49−61%; (b) LiOH, THF, H_2O, rt, 12 h, 93−100%; (c) NH_4Cl, HBTU, DIPEA, DMF, rt, 12 h, 78−81%; (d) $LiAlH_4$, THF, 0 °C, rt 2 h then 70 °C 12 h; (e) 3-({2-[2-(2-{[(*tert*-butoxy)carbonyl]amino}ethoxy)ethoxy]ethyl}carbamoyl)-propanoic acid, HBTU, DIPEA, DMF, rt, 5 h, 34−37%; (f) Ac_2O, Et_3N, CH_2Cl_2, rt, 12 h then NaOH, MeOH, rt, 3 h, 36−37%; (g) $(Boc)_2O$, Et_3N, CH_2Cl_2, 0 °C then rt, 12 h, 33%; (h) TFA, CH_2Cl_2, 0 °C then rt, 2 h, 100%; (i) BODIPY-FL-SE or BODIPY-630/650-SE or Cy5-SE, DIPEA, DMF, rt, 12 h, 14−100%.

DOI: 10.1021/acsmedchemlett.8b00597
ACS Med. Chem. Lett. 2019, 10, 209−214

benzylamines **14** and **15**, respectively, which were not purified prior to subsequent reactions. Primary acetylamines **18** and **19** were synthesized via reaction of **14** and **15** with acetic anhydride, which provided a mixture of *N*,*O*-diacetylated and *N*-acetylated products (by MS and ^{1}H NMR spectroscopy). This mixture was subjected to alkaline hydrolysis to give *N*-acetylated **18** and **19**, respectively. To prepare the shortest BODIPY-FL ligand (**20**), **14** was Boc-protected, purified by silica gel column chromatography, and Boc-deprotected, and the resulting amine was reacted with BODIPY-FL-SE to give **20**. Coupling of **14** or **15** with a PEG2-linked carboxylic acid using HBTU afforded **16** or **17**. Boc-deprotection of **17** followed by reaction with commercially available BODIPY-630/650-SE gave the only benzylic 3-position fluorescent ligand **22**.

Similarly, Boc-deprotection of **16** followed by coupling with commercially available BODIPY-630/650-SE, BODIPY-FL-SE, or Cy5-SE provided fluorescent ligands **21**, **23**, and **24** respectively.

Similarly to the preparation of **20**, **14** underwent several steps to give the longer PEG5-linked **25** (Scheme 2). Linker

Scheme 2. Synthesis of *N*-Phenyl-chromenopyrazole Fluorescent Ligands from Longer Linker Precursors[a]

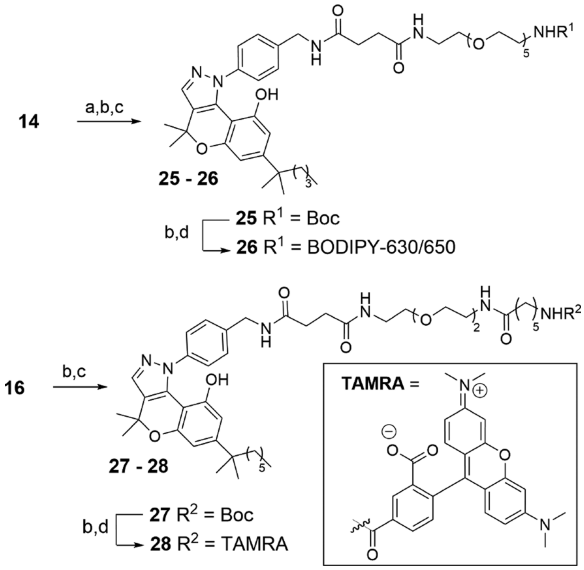

[a]Reagents and conditions: (a) $(Boc)_2O$, Et_3N, CH_2Cl_2, 0 °C then rt, 12 h, 35%; (b) TFA, CH_2Cl_2, 0 °C then rt, 2−3 h, 100%; (c) 3-[(17-{[(*tert*-butoxy)carbonyl]amino}-3,6,9,12,15-pentaoxaheptadecan-1-yl)carbamoyl] propanoic acid or 6-(Boc-amino)hexanoic acid, TFFH, Et_3N, CH_2Cl_2, rt, 12 h, 25−34%; (d) BODIPY-630/650-SE or TAMRA-SE, DIPEA, DMF, rt, 12 h, 100%.

conjugate **25** was Boc-deprotected then reacted with BODIPY630/650-SE to give **26**. The PEG2-linked **16** was further extended by Boc-deprotection and coupling to 6-(Boc-amino)hexanoic acid to afford **27**. Boc-deprotection of **27** and coupling to TAMRA-SE gave fluorescent ligand **28**.

The chromenopyrazoles (**8**−**10**, **16**−**24**, **26**, and **28**) were screened in a competition radioligand binding assay to determine the percentage displacement of [^{3}H]-CP55,940 from CBRs. Compounds that displaced [^{3}H]-CP55,940 by more than 50% at 10 μM (none at CB_1R and 12 out of 14 at CB_2R) were then further analyzed to determine concentration response curves and calculate binding affinity (pK_i). All of the chromenopyrazoles, apart from carboxylic acid **10** and BODIPY-630/650-containing **22**, exhibited moderate to high affinity at CB_2R and were selective over CB_1R (Table 1). Of the *N*-phenyl chromenopyrazoles without linkers (**8**−**10**, **18**, **19**), methylamino-acetyl **18** had the highest affinity and selectivity for CB_2R (pK_i = 7.91 ± 0.10 at hCB_2R; <5.30 at hCB_1R). Chromenopyrazole **18** had a higher affinity for CB_2R than any phenolic chromenopyrazoles previously reported (e.g., **3**−**5**, Figure 1).[21,22] From the three instances of nonfluorescent 3- and 4-position analogues (**8** and **9**, **16** and **17**, **18** and **19**) there was either little difference (**8**, **9**) or a higher CB_2R affinity with the 4-position. For example, the 4-position PEG2-linked **16** (pK_i = 6.87 ± 0.25 at hCB_2R; <5.30 at hCB_1R) exhibited higher affinity for CB_2R than the analogous 3-linked **17**.

The two chromenopyrazoles containing a Boc-protected linker (**16**, **17**) both showed a reduction in CB_2R affinity compared to their truncated equivalents (**18**, **19**). Disappointingly, the presence of the BODIPY-630/650 resulted in a further drop in affinity for CB_2R. While the 4-position BODIPY 630/650 **21** (pK_i = 5.80 ± 0.12 at hCB_2R) was slightly better than the 3-position analogue **22** (pK_i < 5.30), neither fluorescent ligand was of high enough affinity to be useful in imaging studies.

Since the 4-position seemed to exhibit slightly better linker tolerance than the 3-position, the 4-position longer-PEG5-linked BODIPY 630/650 ligand **26** was analyzed to determine whether placing the fluorophore further away from the core ligand would be beneficial. This made little difference as shorter analogue **21** and longer analogue **26** had within experimental error equivalent affinities for CB_2R. BODIPY-FL-containing fluorescent ligand **23** (pK_i = 6.84 ± 0.04 at hCB_2R) showed an increase (~10-fold) in CB_2R affinity compared to the larger sized fluorophore and comparable linker length analogue BODIPY 630/650-**21**. This indicated that a smaller fluorophore in this position may be better tolerated at CB_2R. A TAMRA fluorophore (**28**, pK_i = 6.04 ± 0.06 at hCB_2R) in an equivalent linker-length position was slightly higher affinity than a BODIPY-630/650 (**21**) but not as high affinity as a BODIPY-FL (**23**). Positioning of the BODIPY-FL fluorophore closer to the 4-methylamino moiety of the chromenopyrazole (**20**, pK_i = 6.18 ± 0.04 at hCB_2R) led to a ~0.7 log unit loss in CB_2R affinity compared to the longer-linked BODIPY-FL-**23**.

Among the fluorescent ligands, Cy5-containing **24** exhibited the highest affinity for CB_2R and selectivity over CB_1R (pK_i = 7.38 ± 0.05 at hCB_2R; 5.26 ± 0.11 at hCB_1R) (Supplementary Figure 1A). This shows the fluorophore has a large influence on affinity since **24** contains the analogous "core" and linker length to **21**, **23**, and **28**. Although difficult to compare directly across different assay types, fluorescent ligand **24** (K_i = 41.8 ± 4.5 nM at hCB_2R; 5857 ± 1265 nM at hCB_1R) appears to have the highest ever reported affinity for CB_2R and selectivity over CB_1R than any previously reported CB_2R fluorescent ligand.[14,15,17]

It is highly desirable to know the functional nature of a probe. Ligand **24**, along with **16**, **18**, and **19** were evaluated using a cAMP BRET assay (Table 1). In most cells, CB_2R is coupled to $G_{\alpha i}$ and, when activated by an agonist, inhibits adenylate cyclase, which consequently decreases cAMP. Ligands **16**, **18**, and **19** all behaved as CB_2R agonists, and of these three ligands, the highest affinity **18** was also the most potent (**18**, pIC_{50} = 7.92 ± 0.09 at hCB_2R). The majority of

DOI: 10.1021/acsmedchemlett.8b00597
ACS Med. Chem. Lett. 2019, 10, 209−214

Table 1. Affinity and cAMP Functional Data of Chromenopyrazoles

ligand	fluorophore	hCB$_2$R pK_i[a]	hCB$_1$R pK_i[a]	hCB$_2$R pEC$_{50}$[b] or pIC$_{50}$[c]	hCB$_2$R E_{max}[d]	hCB$_2$R function	hCB$_2$R selectivity[f]
8		6.37 ± 0.06	<5.30	-	-		>12
9		6.57 ± 0.06	<5.30	-	-		>19
10		<5.30	<5.30	-	-		-
16		6.87 ± 0.25	<5.30	6.47 ± 0.03[b]	49.91 ± 3.94	agonist	>37
17		5.90 ± 0.03	<5.30	-	-		>4
18		7.91 ± 0.10	<5.30	7.92 ± 0.09[b]	59.9 ± 2.04	agonist	>407
19		6.41 ± 0.04	<5.30	6.74 ± 0.03[b]	70.36 ± 2.67	agonist	>13
20	BODIPY-FL	6.18 ± 0.04	<5.30	-	-		>8
21	BODIPY-630/650	5.80 ± 0.12	<5.30	-	-		>3
22	BODIPY-630/650	<5.30	<5.30	-	-		-
23	BODIPY-FL	6.84 ± 0.04	<5.30	-	-		>34
24	Cy5	7.38 ± 0.05	5.26 ± 0.11	6.93 ± 0.04[c,e]	176.48 ± 11.85[e]	inverse agonist	131
26	BODIPY-630/650	5.78 ± 0.10	<5.30	-	-		>3
28	TAMRA	6.04 ± 0.06	<5.30	-	-		>6
CP55,940		8.79 ± 0.10	8.34 ± 0.22	8.76 ± 0.05[b]	43.33 ± 0.75	agonist	3
SR144528		7.29 ± 0.03[g]	5.40 ± 0.2[g]	6.28 ± 0.06[c]	148.3 ± 14.17	inverse agonist	78

[a]pK_i obtained by competition binding assay performed with [^{3}H]-CP55,940 (K_d = 1.7 nM hCB$_2$R, K_d = 3.0 nM hCB$_1$R) on hCB$_2$R or hCB$_1$R membrane preparations; data is from at least three individual experiments performed in triplicate. [b]Potency (pEC$_{50}$) [c]or (pIC$_{50}$)) and [d]efficacy (E_{max}) obtained by a cAMP BRET assay using hCB$_2$R-HEK-293 cells; data normalized to forskolin response (100%) and vehicle response (0%); data is from at least three individual experiments performed in duplicate. Inverse agonism is suggested by E_{max} > 100%. '-' indicates data not measured. [e]Efficacy and potency of **24** are an estimate as the concentration response curve was not robustly defined within the concentration range tested (only up to 1 μM was tested due to cAMP assay quenching; see Supplementary Figure 2. [f]hCB$_2$R selectivity: 10 × exp(pK_i hCB$_2$R − pK_i hCB$_1$R). [g]Data obtained from literature.[17] All data is expressed as mean ± SEM.

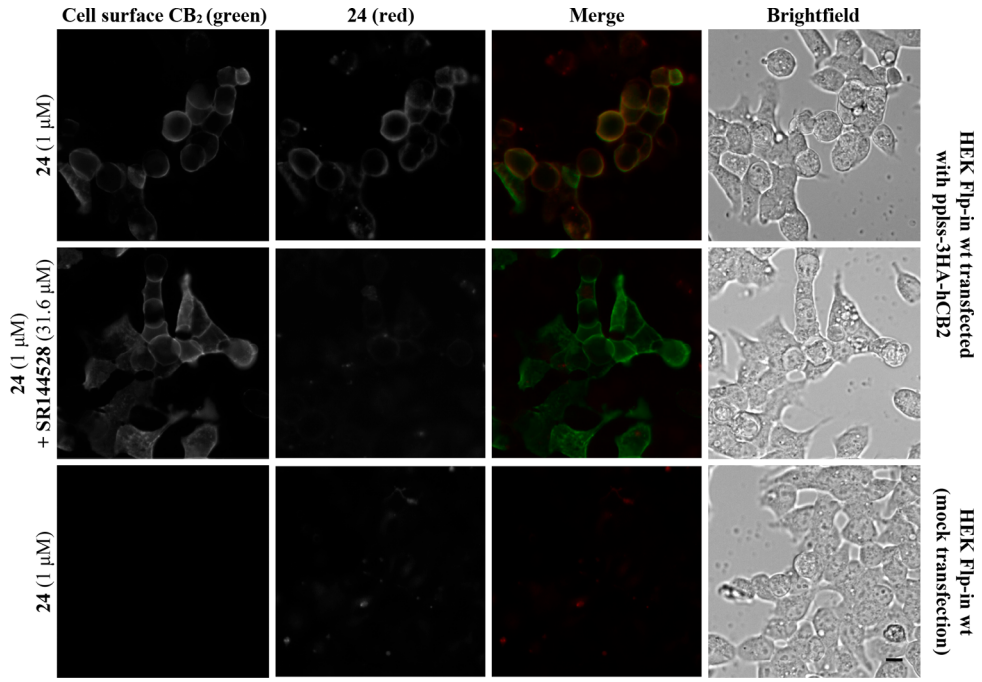

Figure 2. Wide-field fluorescence microscopy images of HEK Flp-in wt cells transiently transfected with pplss-3HA-hCB$_2$R or mock-transfected, preincubated with SR144528 or vehicle for 30 min, then treated with **24** and vehicle or **24** and SR144528 (2 min followed by three washes). Cell surface CB$_2$R was visualized with mouse anti-HA primary antibody and Alexa 488-conjugated goat antimouse secondary antibody. Scale bar = 10 μm. Images representative of three experiments.

previously developed chromenopyrazoles were also reported as agonists at CB$_2$R and/or CB$_1$R.[21,22]

In contrast to **16**, **18**, and **19**, Cy5 ligand **24** behaved as a CB$_2$R inverse agonist in the cAMP BRET assay, and **24** was estimated to exhibit greater efficacy (E_{max} = 176.48 ± 11.85% of forskolin response) and potency (pIC$_{50}$ = 6.93 ± 0.04) than the commonly used reference CB$_2$R inverse agonist SR144528 (Supplementary Figure 1B). Significant interference in the inverse BRET ratio, including that of the vehicle, was observed when using **24** at 10 μM (Supporting Information) as the excitation spectrum of Cy5 partially overlaps with the emission spectrum of YFP.

Therefore, 1 μM was the highest concentration of **24** used in the cAMP BRET assay, and the calculated potency (pIC$_{50}$) and efficacy (E_{max}) of **24** are therefore an estimate due to the concentration response curve not being robustly defined within

DOI: 10.1021/acsmedchemlett.8b00597
ACS Med. Chem. Lett. 2019, 10, 209−214

the concentration range tested. Ligands **16**, **18**, **19**, and **24** were also analyzed for functional response in wild type HEK-293 cells (Supporting Information). Ligands **16**, **18**, and **19** did not show a significant difference to the forskolin-only response; however, **24** did, likely predominantly due to Cy5 interference in the cAMP assay (refer to Supporting Information for discussion).

In addition to high receptor affinity and subtype selectivity, a useful fluorescent ligand also needs to possess suitable physicochemical properties and low nonspecific binding/interactions (for example, with membrane). Wide-field fluorescence microscopy imaging experiments were carried out to determine the ability of **24** to identify CB_2R at a single cell level. Incubation of CB_2R expressing HEK-293 cells with 1 μM of fluorescent ligand **24** exhibited clear cell surface labeling with no detectable intracellular accumulation (Figure 2, Supplementary Figure 4). Specific CB_2R binding of **24** was evident as there was only very low fluorescence observed when the cells were coincubated with high affinity, nonfluorescent CB_2R inverse agonist SR144528 (30 μM), and **24**. CB_2R-specific binding was also evident by the very low amount of fluorescence observed upon incubation of **24** with HEK-293 cells transfected with an empty vector (i.e., lacking CB_2R). As **24** is an inverse agonist, it would be highly unlikely to internalize the receptor, and based on the physicochemical properties of **24** such as large molecular weight and large polar surface area (Supplementary Table 1), it seems unlikely that it would be readily cell permeable. Surface CB_2R-restricted labeling was indicated in our imaging experiments by clear colocalization with cell surface CB_2R (as detected by a noncell-permeable primary antibody directed to an extracellular epitope tag on the receptor) and lack of intracellular labeling, despite CB_2R also being expressed intracellularly in the absence of ligand stimulation (for example, see ref 26). Based on the high CB_2R affinity, selectivity, potent inverse agonist activity, and suitable imaging properties, fluorescent ligand **24** will likely serve as a valuable *in vitro/ex vivo* tool, in particular for studying CB_2R expression in whole cell binding applications.

■ ASSOCIATED CONTENT

Supporting Information

The Supporting Information is available free of charge on the ACS Publications website at DOI: 10.1021/acsmedchemlett.8b00597.

Experimental details of synthesis, assays, and imaging experiments (PDF)

■ AUTHOR INFORMATION

Corresponding Author

*(A.J.V.) Phone: +6434794518. E-mail: andrea.vernall@otago.ac.nz.

ORCID

Andrea J. Vernall: 0000-0001-8056-0726

Present Address

[‖]Department of Pharmacology and Toxicology, University of Otago, Dunedin 9016, New Zealand.

Author Contributions

A.J.V. coordinated and oversaw the project. A.J.V. and S.S. designed the compounds. S.S. carried out the synthesis, radioligand binding, and cAMP assays. C.M. assisted with the pharmacological assays. M.G. advised and supervised the biological experiments. N.L.G. and C.R.O. carried out the imaging experiments. All authors contributed to the writing of the manuscript and have given approval to the final version of the manuscript.

Funding

This work was supported by a University of Otago Research Grant, an Otago Medical Research Foundation Research Grant, and a New Zealand Pharmacy Education and Research Foundation Grant. S.S. was supported by a School of Pharmacy, University of Otago Doctoral Scholarship.

Notes

The authors declare no competing financial interest.

■ ABBREVIATIONS

CB_1R, cannabinoid type 1 receptor; CB_2R, cannabinoid type 2 receptor; GPCR, G protein-coupled receptor; BRET, bioluminescence resonance energy transfer; BODIPY-630/650, (*E*)-6-(2-(4-(2-(5,5-difluoro-7-(thiophen-2-yl)-5*H*-5λ^4,6λ^4-dipyrrolo[1,2-*c*:2′,1′-*f*][1,3,2]diazaborinin-3-yl)vinyl)-phenoxy)acetamido)hexanoyl; BODIPY-FL, 5-(5,5-difluoro-7,9-dimethyl-5*H*-5λ^4,6λ^4-dipyrrolo[1,2-*c*:2′,1′-*f*][1,3,2]-diazaborinin-3-yl)pentanoyl; Cy5, 1-(5-carboxypentyl)-3,3-dimethyl-2-((1*E*,3*E*)-5-((*E*)-1,3,3-trimethylindolin-2-ylidene)-penta-1,3-dien-1-yl)-3*H*-indol-1-ium; DIPEA, *N*,*N*-diisopropylethylamine; HATU, 1-[Bis(dimethylamino)methylene]-1*H*-1,2,3-triazolo[4,5-*b*]pyridinium 3-oxid hexafluorophosphate; HBTU, (2-(1*H*-benzotriazol-1-yl)-1,1,3,3-tetramethyluronium hexafluorophosphate; PEG, polyethylene glycol; TAMRA, 2-(3,6-bis(dimethylamino)xanthylium-9-yl)-5-carboxybenzoate; TFFH, tetramethylfluoroformamidinium hexafluorophosphate; SE, succinimidyl ester

■ REFERENCES

(1) Pertwee, R. G.; Howlett, A. C.; Abood, M. E.; Alexander, S. P. H.; Di Marzo, V.; Elphick, M. R.; Greasley, P. J.; Hansen, H. S.; Kunos, G.; Mackie, K.; Mechoulam, R.; Ross, R. A. International Union of Basic and Clinical Pharmacology. LXXIX. Cannabinoid Receptors and Their Ligands: Beyond CB1 and CB2. *Pharmacol. Rev.* **2010**, *62*, 588−631.

(2) Pacher, P.; Bátkai, S.; Kunos, G. The Endocannabinoid System as an Emerging Target of Pharmacotherapy. *Pharmacol. Rev.* **2006**, *58*, 389−462.

(3) Turcotte, C.; Blanchet, M.-R.; Laviolette, M.; Flamand, N. The CB2 Receptor and Its Role as a Regulator of Inflammation. *Cell. Mol. Life Sci.* **2016**, *73*, 4449−4470.

(4) Shang, Y.; Tang, Y. The Central Cannabinoid Receptor Type-2 (CB2) and Chronic Pain. *Int. J. Neurosci.* **2017**, *127*, 812−823.

(5) Morales, P.; Hernandez-Folgado, L.; Goya, P.; Jagerovic, N. Cannabinoid receptor 2 (CB2) agonists and antagonists: A patent update. *Expert Opin. Ther. Pat.* **2016**, *26*, 843−856.

(6) Cooper, A.; Singh, S.; Hook, S.; Tyndall, J. D. A.; Vernall, A. J. Chemical Tools for Studying Lipid-Binding Class A G Protein−Coupled Receptors. *Pharmacol. Rev.* **2017**, *69*, 316−353.

(7) Martella, A.; Sijben, H.; Rufer, A. C.; Grether, U.; Fingerle, J.; Ullmer, C.; Hartung, T.; IJzerman, A. P.; van der Stelt, M.; Heitman, L. H. A Novel Selective Inverse Agonist of the CB_2 Receptor as a Radiolabeled Tool Compound for Kinetic Binding Studies. *Mol. Pharmacol.* **2017**, *92*, 389−400.

(8) Marchalant, Y.; Brownjohn, P. W.; Bonnet, A.; Kleffmann, T.; Ashton, J. C. Validating Antibodies to the Cannabinoid CB2 Receptor: Antibody Sensitivity Is Not Evidence of Antibody Specificity. *J. Histochem. Cytochem.* **2014**, *62*, 395−404.

DOI: 10.1021/acsmedchemlett.8b00597
ACS Med. Chem. Lett. 2019, 10, 209−214

(9) Stoddart, L. A.; Kilpatrick, L. E.; Briddon, S. J.; Hill, S. J. Probing the pharmacology of G protein-coupled receptors with fluorescent ligands. *Neuropharmacology* **2015**, *98*, 48−57.
(10) Vernall, A. J.; Hill, S. J.; Kellam, B. The evolving small-molecule fluorescent-conjugate toolbox for Class A GPCRs. *Br. J. Pharmacol.* **2014**, *171*, 1073−1084.
(11) Lam, R.; Gondin, A. B.; Canals, M.; Kellam, B.; Briddon, S. J.; Graham, B.; Scammells, P. J. Fluorescently Labeled Morphine Derivatives for Bioimaging Studies. *J. Med. Chem.* **2018**, *61*, 1316−1329.
(12) Iliopoulos-Tsoutsouvas, C.; Kulkarni, R. N.; Makriyannis, A.; Nikas, S. P. Fluorescent probes for G-protein-coupled receptor drug discovery. *Expert Opin. Drug Discovery* **2018**, *13*, 933.
(13) Stoddart, L. A.; Kilpatrick, L. E.; Hill, S. J. NanoBRET Approaches to Study Ligand Binding to GPCRs and RTKs. *Trends Pharmacol. Sci.* **2018**, *39*, 136−147.
(14) Sexton, M.; Woodruff, G.; Horne, E. A.; Lin, Y. H.; Muccioli, G. G.; Bai, M.; Stern, E.; Bornhop, D. J.; Stella, N. NIR-mbc94, a fluorescent ligand that binds to endogenous CB_2 receptors and is amenable to high-throughput screening. *Chem. Biol.* **2011**, *18*, 563−568.
(15) Zhang, S.; Shao, P.; Bai, M. In vivo type 2 cannabinoid receptor-targeted tumor optical imaging using a near infrared fluorescent probe. *Bioconjugate Chem.* **2013**, *24*, 1907−1916.
(16) Cooper, A. G.; MacDonald, C.; Glass, M.; Hook, S.; Tyndall, J. D. A.; Vernall, A. J. Alkyl indole-based cannabinoid type 2 receptor tools: Exploration of linker and fluorophore attachment. *Eur. J. Med. Chem.* **2018**, *145*, 770−789.
(17) Cooper, A. G.; Oyagawa, C. R. M.; Manning, J. J.; Singh, S.; Hook, S.; Grimsey, N. L.; Glass, M.; Tyndall, J. D. A.; Vernall, A. J. Development of Selective, Fluorescent Cannabinoid Type 2 Receptor Ligands Based on a 1,8-Naphthyridin-2-(1 H)-One-3-Carboxamide Scaffold. *MedChemComm* **2018**, *9*, 2055−2067.
(18) Soethoudt, M.; Stolze, S. C.; Westphal, M. V.; van Stralen, L.; Martella, A.; van Rooden, E. J.; Guba, W.; Varga, Z. V.; Deng, H.; van Kasteren, S. I.; Grether, U.; Ijzerman, A. P.; Pacher, P.; Carreira, E. M.; Overkleeft, H. S.; Ioan-Facsinay, A.; Heitman, L. H.; van der Stelt, M. Selective Photoaffinity Probe That Enables Assessment of Cannabinoid CB2 Receptor Expression and Ligand Engagement in Human Cells. *J. Am. Chem. Soc.* **2018**, *140*, 6067−6075.
(19) Martín-Couce, L.; Martín-Fontecha, M.; Palomares, Ó.; Mestre, L.; Cordomí, A.; Hernangomez, M.; Palma, S.; Pardo, L.; Guaza, C.; López-Rodríguez, M. L.; Ortega-Gutiérrez, S. Chemical Probes for the Recognition of Cannabinoid Receptors in Native Systems. *Angew. Chem., Int. Ed.* **2012**, *51*, 6896−6899.
(20) Martín-Fontecha, M.; Angelina, A.; Rückert, B.; Rueda-Zubiaurre, A.; Martín-Cruz, L.; van de Veen, W.; Akdis, M.; Ortega-Gutiérrez, S.; López-Rodríguez, M. L.; Akdis, C. A.; Palomares, O. A Fluorescent Probe to Unravel Functional Features of Cannabinoid Receptor CB1 in Human Blood and Tonsil Immune System Cells. *Bioconjugate Chem.* **2018**, *29*, 382−389.
(21) Cumella, J.; Hernandez-Folgado, L.; Giron, R.; Sanchez, E.; Morales, P.; Hurst, D. P.; Gomez-Canas, M.; Gomez-Ruiz, M.; Pinto, D.; Goya, P.; Reggio, P. H.; Martin, M. I.; Fernandez-Ruiz, J.; Silva, A. M. S.; Jagerovic, N. Chromenopyrazoles: Non-psychoactive and Selective CB1 Cannabinoid Agonists with Peripheral Antinociceptive Properties. *ChemMedChem* **2012**, *7*, 452−463.
(22) Morales, P.; Gómez-Cañas, M.; Navarro, G.; Hurst, D. P.; Carrillo-Salinas, F. J.; Lagartera, L.; Pazos, R.; Goya, P.; Reggio, P. H.; Guaza, C.; Franco, R.; Fernández-Ruiz, J.; Jagerovic, N. Chromenopyrazole, a Versatile Cannabinoid Scaffold with in Vivo Activity in a Model of Multiple Sclerosis. *J. Med. Chem.* **2016**, *59*, 6753−6771.
(23) Morales, P.; Goya, P.; Jagerovic, N. The chromenopyrazole scaffold in the modulation of the endocannabinoid system: A broad therapeutic prospect. *Anal. Real Acad. Nac. F.* **2018**, *84*, 164−184.
(24) Morales, P.; Moreno, L.; Fernández-Ruiz, J.; Jagerovic, N. Synthesis of a novel CB2 cannabinoid-porphyrin conjugate based on an antitumor chromenopyrazoledione. *J. Porphyrins Phthalocyanines* **2017**, *21*, 67−76.
(25) Vernall, A. J.; Stoddart, L. A.; Briddon, S. J.; Ng, H. W.; Laughton, C. A.; Doughty, S. W.; Hill, S. J.; Kellam, B. Conversion of a non-selective adenosine receptor antagonist into A3-selective high affinity fluorescent probes using peptide-based linkers. *Org. Biomol. Chem.* **2013**, *11*, 5673−5682.
(26) Kleyer, J.; Nicolussi, S.; Taylor, P.; Simonelli, D.; Furger, E.; Anderle, P.; Gertsch, J. Cannabinoid receptor trafficking in peripheral cells is dynamically regulated by a binary biochemical switch. *Biochem. Pharmacol.* **2012**, *83*, 1393−1412.

DOI: 10.1021/acsmedchemlett.8b00597
ACS Med. Chem. Lett. 2019, 10, 209−214